Translocation of a Single-Stranded DNA Through a Conformationally Changing Nanopore

O. Flomenbom and J. Klafter
School of Chemistry, Raymond and Beverly Sackler Faculty of Exact Sciences, Tel Aviv University, Tel Aviv, Israel

ABSTRACT We investigate the translocation of a single-stranded DNA through a pore which fluctuates between two conformations, using coupled master equations. The probability density function of the first passage times of the translocation process is calculated, displaying a triple-, double-, or monopeaked behavior, depending on the interconversion rates between the conformations, the applied electric field, and the initial conditions. The cumulative probability function of the first passage times, in a field-free environment, is shown to have two regimes, characterized by fast and slow timescales. An analytical expression for the mean first passage time of the translocation process is derived, and provides, in addition to the interconversion rates, an extensive characterization of the translocation process. Relationships to experimental observations are discussed.

INTRODUCTION

Translocation of biopolymers through a membrane pore occurs in a variety of biological processes, such as gene expression in eukaryotic cells (Alberts et al., 1994), conjugation between prokaryotic cells, and virus infection (Madigan et al., 1997). The importance of translocation in biological systems and its applications have been the motivation for recent theoretical and experimental work on this topic. In experiments one usually measures the time it takes one voltage-driven single-stranded DNA (ssDNA) to translocate through the α-hemolysin channel of a known structure (Song et al., 1996). Since ssDNA is negatively charged (each monomer of length b has an effective charge of zq, where q is the electron charge, and z, i.e., $0 < z < 1$, is controlled by the solution pH and strength), when applying a voltage the polymer is subject to a driving force while passing through the transmembrane pore part (TPP) from the negative (*cis*) side to the positive (*trans*) side; for an illustration of the process, see Fig. 4 in Meller (2003). Because the presence of the ssDNA in the TPP blocks the cross-TPP current, one can deduce the first passage times (FPT) probability density function (pdf), $F(t)$, from the current blockade duration times (Kasianowicz et al., 1996; Meller et al., 2001).

Experiments by Kasianowicz et al. (1996) show $F(t)$ with three peaks. It was suggested that the short-time peak represents the nontranslocated events, whereas the other two, longer-time peaks, represent translocation events of different ssDNA orientations. In addition, the times that maximize the translocation peaks were shown to be proportional to the polymer length and inversely proportional to the applied field. In experiments by Meller et al. (2001), $F(t)$ was shown to be monopeaked, with a corresponding maximizing time characterized by an inverse quadratic field dependence. More recently, Bates et al. (2003) measured the FPT cumulative probability density function (cdf), which is the probability to exit the channel until time t, $G(t) = \int_0^t F(s)ds$ in a field-free environment. $G(t)$ was approximated by two well-separated timescales with the ratio of 1:20.

In previous theoretical works, the translocation of a ssDNA through a nanopore was described by statistical models that focused on calculating the free energy of the process as a function of the translocation state. The free energy contained terms representing the entropy and the chemical potential of the polymer parts on both sides of a zero-thickness membrane (Muthukumar, 1999; Sung and Park, 1996). The role of the membrane thickness was studied by Ambjornsson et al. (2002), Slonika and Kolomeisky (2003), and Flomenbom and Klafter (2003). The effects of the sequence of the ssDNA on the translocation were considered by Flomenbom and Klafter (2003), Kafri et al. (2004), and Slutsky et al. (2004). The obtained free energy was mainly used to calculate the mean first passage time (MFPT), which asymptotically was found to scale linearly with the polymer length for a field-biased process. This is the expected MFPT dependence of a Markovian-biased random walk in a finite interval (Redner, 2001).

A different approach was suggested by Lubensky and Nelson (2001), and further developed by Berezhkovskii and Gopich (2003), where a diffusion-convection equation was used to describe the translocation process, under the assumption that the polymer parts outside the membrane hardly affect the translocation. Berezhkovskii and Gopich (2003) showed that by changing the *cis* absorbing end to be partially absorbing, the monopeaked $F(t)$ obtained by Lubensky and Nelson (2001) could change to a superposition of a decaying nontranslocation pdf and a peaked translocation pdf. Chuang et al. (2001) studied a field-free translocation which they described by Rouse dynamics, which was shown to yield anomalous scaling laws of the

Submitted December 8, 2003, and accepted for publication March 1, 2004.

Address reprint requests to Ophir Flomenbom, Tel Aviv University, Chemical Physics, Raymond and Beverly Sackler Faculty of Exact Sciences, Tel Aviv 69978, Israel. Tel.: 972-3-640-7229; E-mail: flomenbo@post.tau.ac.il.

0006-3495/04/06/3576/09 $2.00

doi: 10.1529/biophysj.103.037580

MFPT. Using the fractional Fokker-Planck equation, Metzler and Klafter (2003) suggested an explanation for the slow relaxation time of the experimentally observed $G(t)$. We have shown by using a master equation (ME) approach that $F(t)$ can be double- or monopeaked, depending on the applied field and on the initial condition (Flomenbom and Klafter, 2003).

In the various approaches summarized above the structure of the pore was taken to be rigid, namely, governed by a single conformation. Although it is known that the α-hemolysin channel has a rigid structure that allows its crystallization (Song et al., 1996), during the translocation of a long polymer (larger than the pore length) which is almost as wide as the channel at some cross sections along it, small fluctuations in the channel structure can occur which may not be relevant to ion movement but which are important to ssDNA translocation. This gives rise to a more complex process than what has been assumed so far. In this work we relax the assumption of a single pore conformation and introduce a second conformation coupled to the first one. The process then takes place in an effectively two-dimensional system, where one dimension represents the translocation itself, and the second dimension represents the structural fluctuations. This picture is richer and is more realistic, since small structural changes in physiological conditions are known to occur in large biomolecules, certainly during interaction with other biomolecules.

The function that best represents the translocation process is $F(t)$ (or its integral $G(t)$). Through the dependence of $F(t)$ on the system parameters we learn about the important degrees of freedom which participate in the translocation process. The characteristics of $F(t)$ are the dependence of its shape, moments, and times that maximize its peaks on the system parameters. Using the generalized model that takes into account fluctuations in the pore structure, we calculate $F(t)$ and show that it can display one, two, or three peaks, depending on the applied voltage, the temperature, and the interconversion rates between the two conformations. Analytical expressions for the MFPT are derived and related to the experimental findings. In addition, we calculate the cumulative probability $G(t)$ in the field-free limit, and show that it also provides valuable information about the system parameters. Thus, these tools help in gaining insight into the translocation of a polymer through a narrow pore, and in explaining the diversity of the experimental observations (Kasianowicz et al., 1996; Meller et al., 2001).

THEORETICAL MODELING

Basic model

The basic model we use to describe the translocation relies on a one-dimensional process. To apply this simplification, we map the three-dimensional translocation process onto a discrete one-dimensional space containing $n(= N + d–1)$ states separated from each other by a unit length b. The translocation takes place within a TPP of a length that corresponds to d-monomers. An n-state ME is introduced to describe the translocation of an N-monomer-long ssDNA subject to an external voltage V and temperature T. The occupation pdf of the j-state is $[\vec{P}(t)]_j = P_j(t)$, where the state index j determines the number of monomers on each side of the membrane and within the TPP (m_j). $P_j(t)$ satisfies the equation of motion

$$\partial P_j(t)/\partial t = a_{j+1,j}P_{j+1}(t) + a_{j-1,j}P_{j-1}(t) - (a_{j,j+1} + a_{j,j-1})P_j(t), \quad (1)$$

under absorbing boundary conditions on both sides of the membrane (the polymer can exit the TPP on both sides). Equation 1 can be written in a matrix representation as

$$\partial \vec{P}(t)/\partial t = \mathbf{A}\vec{P}(t), \quad (2)$$

where the propagation matrix $\mathbf{A}$ is a tridiagonal matrix that contains information about the transitions between states in terms of rate constants, $a_{j,j\pm1}$, which is given by

$$a_{j,j\pm1} = k_j p_{j,j\pm1}. \quad (3)$$

Here, k_j is the rate to perform a step, $p_{j,j-1}$ ($p_{j,j+1}$) is the probability to move one state from state j to the *trans* (*cis*) side, and $p_{j,j+1} + p_{j,j-1} = 1$. The expression for k_j is taken to be similar to the longest bulk relaxation time of a polymer (Doi and Edwards, 1986),

$$k_j = 1/(\beta\xi_p b^2 m_j^\mu) \equiv R/m_j^\mu; \quad \beta^{-1} \equiv k_B T, \quad (4)$$

with two exceptions: the parameter ξ_p represents the ssDNA-TPP interaction and cannot be calculated from the Stokes relation, and μ serves as a measure of the polymer stiffness inside the confined volume of the TPP, and is bounded by the conventional values (Doi and Edwards, 1986) of $0 \le \mu \le 1.5$.

Assuming a quasiequilibrium process, which justifies applying the detailed balance condition, and by using the approximation $a_{j,j-1}/a_{j-1,j} \approx p_{j,j-1}/(1-p_{j,j-1})$, the probability $p_{j,j-1}$ is found to be

$$P_{j,j-1} = (1 + e^{\beta\Delta E_j})^{-1}. \quad (5)$$

The free energy difference between states, $\Delta E_j = E_{j-1} - E_j$, is computed considering three contributions: electrostatic, entropic, and an average attractive interaction energy between the ssDNA and the pore. More explicitly, $\beta\Delta E_j$ is given by $\beta\Delta E_j = \beta\Delta E_j^P + \delta_j$, where $\beta\Delta E_j^P \le 0$ represents the effect of the field which directs toward the *trans*-side and

$\delta_j > 0$ (for $j > d$) represents an effective directionality to the *cis*-side, which originates from the entropic factors and the average attractive interaction energy between the ssDNA and the pore. For a more detailed discussion see Flomenbom and Klafter (2003).

Several features emerge from the simple one-dimensional model. For homopolymers, poly-*dnu*, where *nu* stands for the nucleotide type, we estimate $\xi_p(A_{nu}) \approx 10^{-4}$meVs/nm^2, $\xi_p(C_{nu}) = \xi_p(T_{nu}) = \xi_p(A_{nu})/3$ and $\mu(C_{nu}) = 1$, $\mu(A_{nu}) = 1.14$, $\mu(T_{nu}) = 1.28$. Here A_{nu}, C_{nu}, and T_{nu} stand for adenine, cytosine, and thymine nucleotides, respectively. Interestingly, ξ_p is three orders-of-magnitude larger than the bulk friction constant, which is consistent with the role assigned to ξ_p to represent the interaction between the polymer and the channel.

In addition, from the expressions for $\beta\Delta E_j$ and $p_{j,j-1}$, the important parameter $V/V_C \equiv \beta z|q|V(1 + 1/d)$ comes out naturally. This ratio determines the directionality of the translocation, and, in particular, for $V/V_C > 1$ there is a bias toward the *trans*-side of the membrane.

Translocation through a conformationally changing pore

A more realistic description of the translocation can be obtained by taking into consideration fluctuations in the TPP, either spontaneous or interaction-induced. Accordingly, we introduce an additional pore conformation which is represented by the propagation matrix **B**. The changes in the pore conformation between *A* and *B* are controlled by the interconversion rates, ω_A and ω_B. The value ω_A (ω_B) is the rate of the change from the *A* (*B*) to the *B* (*A*) pore conformation.

The physical picture of the process is that when the pore conformation changes, a different environment is created for the ssDNA occupying the TPP. This implies a change in ξ_p and μ. For a large polymer, $N > d$, we take $\mathbf{B} \approx \lambda\mathbf{A}$, where λ is a (dimensionless) parameter that represents the effect of the conformational change on ξ_p and μ (as stems from Eq. 4 and the relationship $\mathbf{B} \approx \lambda\mathbf{A}$). The parameter λ may be interpreted as a measure of the effective available volume created within the TPP when the amino acid residues protruding the TPP change their positions.

The equations of motion of the ssDNA translocation through the fluctuating pore, written in matrix representation, are

$$\frac{\partial}{\partial t}\begin{pmatrix}\vec{P}(t;A)\\ \vec{P}(t;B)\end{pmatrix} = \begin{pmatrix}\mathbf{A}-\boldsymbol{\omega}_\mathbf{A} & \boldsymbol{\omega}_\mathbf{B}\\ \boldsymbol{\omega}_\mathbf{A} & \mathbf{B}-\boldsymbol{\omega}_\mathbf{B}\end{pmatrix}\begin{pmatrix}\vec{P}(t;A)\\ \vec{P}(t;B)\end{pmatrix}, \quad (6)$$

where $\vec{P}(t;i), i = A,B$ is the occupation pdf vector of conformation i, $\omega_i = \omega_i\mathbf{I}$, and $\mathbf{I}$ is the unit matrix of n dimensions. For the reader's convenience, Table 1, which summarizes the important parameters of the model and the calculated entities, is given in Appendix E.

As a general note we refer to the form of Eq. 6, which was used to study the resonant activation phenomenon (Bar-Haim and Klafter, 1999). This phenomenon, which was first reported by Doering and Gadoua (1992), is the occurrence of a global minimum in the MFPT as a function of the interconversion rate for a system in which $\omega_A = \omega_B$. Because of the assumption $\mathbf{B} = \lambda\mathbf{A}$, the system investigated here cannot exhibit this phenomenon (Flomenbom and Klafter, 2004).

DENSITY OF TRANSLOCATION TIMES

Parameter tuning

To study the translocation of ssDNA through a fluctuating pore, we start by computing $F(t)$. Formally, $F(t)$ is defined by

$$F(t) = \partial(1 - S(t))/\partial t. \quad (7)$$

Here, $S(t)$ is the survival probability; namely, the probability to still have at least one monomer in the pore, and which is given by summing the elements of the vector that solves Eq. 6 (see Appendix A for details). Using the values of ξ_p and μ from the single conformation model, we examine in this subsection the effect of the parameters λ, ω_A, and ω_B on $F(t)$.

First, we check the effect of λ on $F(t)$ for several limiting cases. For $\lambda = 0$ movement in any direction occurs only under the *A* conformation environment. The *B* conformation traps the polymer for a period of time governed by the interconversion rates. For $\lambda = 1$, namely, $\mathbf{B} = \mathbf{A}$, the environmental changes do not affect the translocation, and the process reduces to a translocation through a single conformation. For $\lambda > 1$ the environmental changes enhance the process. In this article we restrict ourselves to the range $0 \le \lambda \le 1$.

The picture is less intuitive for intermediate values of λ. Fig. 1 shows that by choosing λ properly, three peaks in $F(t)$ can be obtained. In particular, as shown in the inset of Fig. 1, the range of λ-values for which $F(t)$ exhibits three distinct peaks is $0.10 \le \lambda \le 0.30$. For the single conformation case we found that $F(t)$ can be either mono- or doublepeaked, depending on V/V_C, and on the initial state of the translocation x. The short time peak represents the nontranslocated events, whereas the long time peak represents the translocation events. The generalization to two pore conformations may yield two translocation peaks in addition to a short time nontranslocation peak. Indeed, Fig. 1 supports the expected behavior for the limiting λ-values, and shows that as $\lambda \to 1$, $F(t)$ possess only one translocation peak, as well as for $\lambda \to 0$, where the *B* conformation peak spreads out toward larger times, which results in its disappearance.

Although Fig. 1 is obtained for a given value of the interconversion rates, our explanations regarding the $F(t)$ behavior for the limiting cases $\lambda = 1, 0$ are valid for any system conditions. This is demonstrated by calculating the MFPT (Appendices B and D). In Appendix B we show that when $\lambda = 1$, the MFPT of the two-conformation model

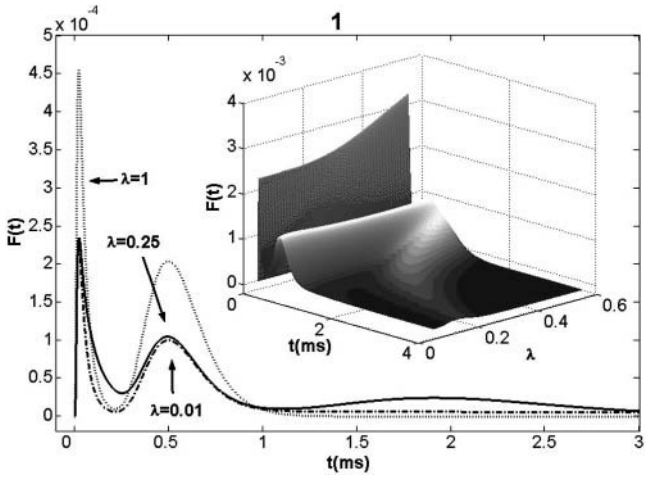

FIGURE 1 Poly-dT_{nu} $F(t)$, for several values of λ, with: $N = 30$, $d = 12$, $x = N + d/2$, $T = 2°C$, $V/V_C = 2$, $\omega_B = 10^2$Hz, $\omega = 1$, and $z \approx 1/2$. The left peak represents the nontranslocated events, whereas the other two peaks represent translocation. (*Inset*) The range for which λ yields three-peaked $F(t)$ is shown to be $0.10 \leq \lambda \leq 0.30$, when given the above parameters.

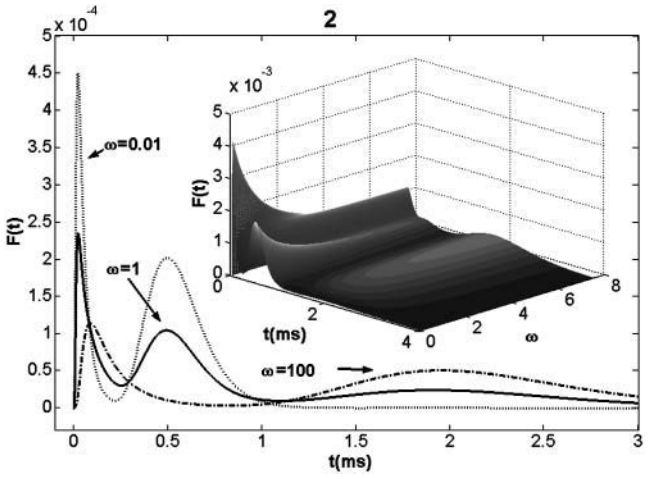

FIGURE 2 Poly-dT_{nu} $F(t)$, for several values of ω_A and fixed ω_B ($\omega_B = 10^2$ Hz), with $\lambda = 1/4$, and the other parameters as in Fig. 1. (*Inset*) For small values of ω, $\omega \lesssim 10^{-2}$, $F(t)$ displays one translocation peak that corresponds to A, whereas for large values of ω, $\omega \gtrsim 10^2$, $F(t)$ displays one translocation peak that corresponds to B. For $\omega \approx 1$, two translocation peaks are obtained.

reduces to that of the single conformation model. In Appendix D we show that for $\lambda = 0$, the B conformation contribution for the MFPT is a term which is inversely proportional to the interconversion rate, ω_B^{-1}.

Therefore, λ serves as a tuning parameter that leads to either one or two actual translocation peaks in $F(t)$. The question of interest is how λ depends on the system parameters. We assume a small field perturbation in the regime of biological interest ($0 \leq V/V_C \leq 3$, using $V_C \approx 50$ mV; Flomenbom and Klafter, 2003), so that $\lambda(V)$ follows $\lambda \approx \lambda_0 + V/V_\lambda$, and keeping $\lambda(V) \leq 1$. Here λ_0 and V_λ might be expansion coefficients, where $\lambda \ll 1$ is implied from recent experiments (Bates et al., 2003), as we discuss later. The process can be viewed in the following way: as the voltage increases, those residues of amino acids that protrude the TPP, creating obstacles for the translocating ssDNA, clear the way. Although the λ-dependence on the voltage is assumed here, its dependence on other system parameters (e.g., temperature and pH) is unknown and is folded into V_λ.

To check how interconversion rates affect $F(t)$, it is convenient to define two dimensionless parameters, $\omega \equiv \omega_A/\omega_B$ and ω_B/k (or ω_A/k), where k is the dominant rate of the A conformation for a sufficiently large N, $k = R/d^\mu$. The first ratio sets the dominance of a given conformation over its counterpart; e.g., for $\omega \ll 1$ most of the translocation events take place in the A conformation. The second ratio gives an estimate of the number of moves in a given conformation before a change in the pore structure occurs, and thus relates the ssDNA dynamics to the structural changes dynamics.

As shown in Fig. 2 and its inset, $F(t)$ exhibits two peaks corresponding to actual translocation only when $\omega \approx 1$. For $\omega \ll 1$ and $\omega \gg 1$ only one peak corresponding to an actual translocation survives. For all cases there is a peak representing nontranslocation events. In addition, we find that for two translocation peaks to be obtained, the ratio ω_B/k (or ω_A/k due to $\omega \approx 1$) must fulfill $\omega_B/k \leq 10^{-3}$ (data not shown). The lower limit for the interconversion rates is inversely proportional to the order of the measurement time, otherwise only one conformation will be detected.

Finally, we assume that the rate of the conformational changes is controlled mainly by temperature; namely, we take ω_A and ω_B as voltage-independent in the regime of biological interest: $0 \leq V/V_C \leq 3$.

Translocation velocity

To study further the translocation process, we check the voltage dependence of the times that maximize the peaks of $F(t)$, denoted as $t_{m,i}$ where $i = 1, 2, 3$ (e.g., $t_{m,1}$ characterized the short time peak). In previous works (Flomenbom and Klafter, 2003; Meller et al., 2001) t_m^{-1} for one translocation peak was regarded as the most probable velocity of the translocation (up to a multiplicative constant). We show below that our assumptions regarding the voltage dependence of the system parameters yield either linear or quadratic dependence of the translocation velocity on the voltage, and can be used to explain the different experimental observations.

Fig. 3 shows $t_{m,i}(V_C/V)$ and $t_{m,i}^{-1}(V/V_C)$, for $V_\lambda = 350$ mV, in a voltage window that leads to $0.215 \leq \lambda(V) \leq 0.30$, and accordingly to a triple-peaked $F(t)$. $t_{m,1}$ is almost independent of V_C/V (see Fig. 3 *a*). Although the nontranslocation peak amplitude decreases upon increasing V/V_C, the location of its maximum hardly changes. This happens since exiting against the field occurs within a short

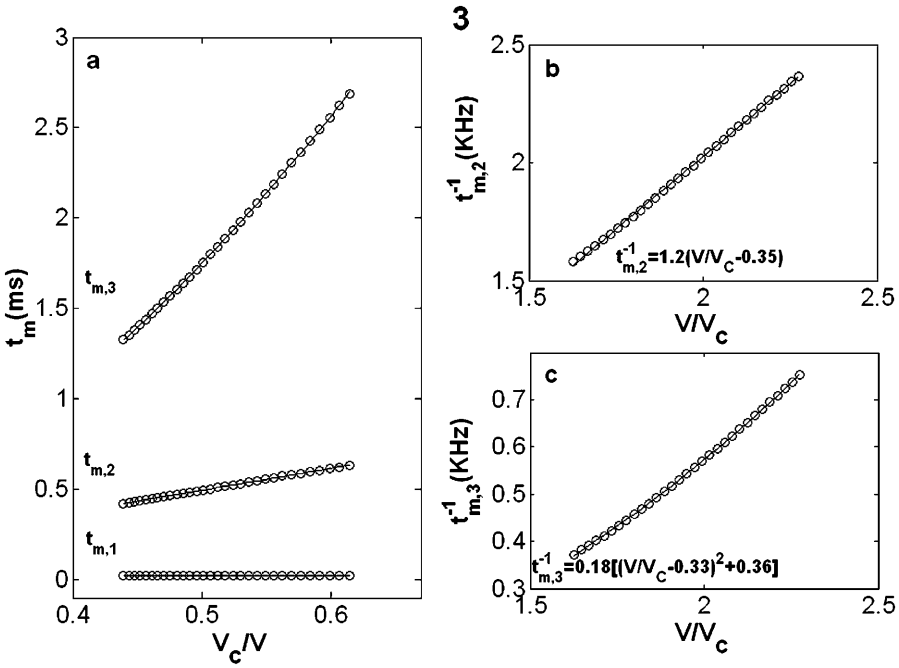

FIGURE 3 (*a*) $t_{\mathrm{m,i}}$ for poly-dT_{nu}, as a function of V_C/V, and the same parameters as in Fig. 1 and $V_\lambda = 350$ mV. $t_{\mathrm{m,1}}$ is almost independent of V_C/V in contrast to the pronounced dependence of $t_{\mathrm{m,2}}$ and $t_{\mathrm{m,3}}$ (*b* and *c*). $t^{-1}_{\mathrm{m,2}}$ and $t^{-1}_{\mathrm{m,3}}$ depend linearly and quadratically on V/V_C, respectively. The solid lines through the circles are polynomial fits.

time window at the beginning of the process, otherwise the polymer is more likely to cross the membrane due to the electric bias. Similar behavior was observed experimentally (Kasianowicz et al., 1996).

For the single conformation case, we showed that $t^{-1}_{\mathrm{m,2}}$ scales linearly with V/V_C when the initial state of the translocation is near the *cis*-side of the membrane (Flomenbom and Klafter, 2003). Fig. 3 *b* shows that the linear scaling of $t^{-1}_{\mathrm{m,2}}(V/V_C)$ persists. However, $t^{-1}_{\mathrm{m,3}}(V/V_C)$ (Fig. 3 *c*) displays a quadratic behavior, which is a consequence of the form of $\lambda(V)$, as discussed in the next section when calculating the MFPT. On the other hand, setting $V_\lambda = 120$ mV leads to one translocation peak, and to small deviations from linearity toward a weak quadratic behavior of $t^{-1}_{\mathrm{m,2}}(V/V_C)$; see Fig. 4.

The model of two conformations not only yields one or two actual translocation peaks as a function of V_λ, but can account for either a linear or quadratic dependence of the translocation velocity with the voltage, again as a function of V_λ. Thus, varying V_λ we obtain different behaviors of the translocation, which can be related to the different experimental observations.

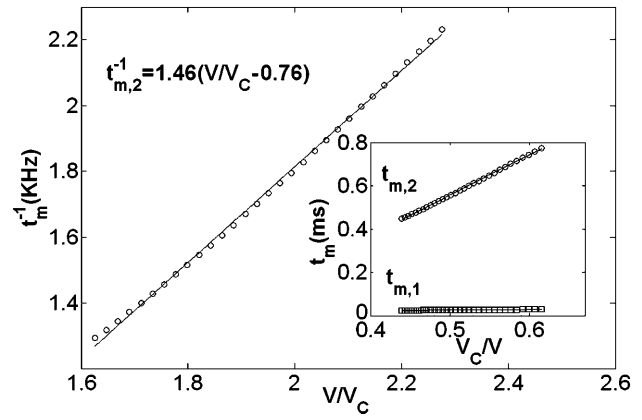

FIGURE 4 $t^{-1}_{m,2}$ for poly-dT_{nu} for the same parameters as in Fig. 3 except for $V_\lambda = 120$ mV. This value for V_λ leads to $0.625 \le \lambda(V) \le 0.875$ and accordingly for one translocation peak. The solid line is a polynomial fit. (*Inset*) $t_{\mathrm{m,1}}$ and $t_{\mathrm{m,2}}$ behave qualitatively the same as for the case $V_\lambda = 350$ mV.

THE MFPT

Small-field biased translocation

We now turn to calculating the MFPT, which allows for an analytical estimation of the characteristic times of the FPT pdf and cdf. In general, the m moment of $F(t)$ is calculated by raising to the m power the inverse of the propagation matrix. For the two conformation translocations this matrix is given on the right-hand side of Eq. 6.

After somewhat lengthy calculations, which are given in Appendices B and C, the expression for the MFPT, $\langle\tau\rangle$, reads

$$\langle\tau\rangle \approx \frac{\bar{\tau}}{\lambda}[(\lambda P_{\mathrm{A},0} + P_{\mathrm{B},0}) + \bar{\tau}(\omega_{\mathrm{A}} + \omega_{\mathrm{B}})/2], \qquad (8)$$

where $\bar{\tau}$ is the MFPT for the single conformation model, and is given by Eq. C5, and $P_{\mathrm{A},0}(P_{\mathrm{B},0})$ is the probability that the

process starts in conformation A (B). For $P_{A,0}$ and $P_{B,0}$ the equilibrium condition is assumed, $P_{A,0} = \omega_B/(\omega_A + \omega_B)$ and $P_{B,0} = 1 - P_{A,0}$.

Equation 8 is valid for not-too-high fields, $V/V_C \gtrsim 1$, and for the ratios between the interconversion rates and k found in the previous section, ω_A/k, $\omega_b/k \ll 1$. The first term in the brackets of Eq. 8, $\lambda P_{A,0} + P_{B,0}$, represents the translocation peaks and can be compared with $t_{m,2}$ and $t_{m,3}$. The second term in the brackets, $\bar{\tau}(\omega_A + \omega_B)/2$, represents the coupling time cost, and is of the order of $o(10^{-2})$ for voltages that obey $V/V_C \geq 1.5$. Keeping the first term in Eq. 8, we have

$$\langle\tau\rangle \approx \frac{2x\xi_p b^2 d^{\mu}}{z|q|(1+1/d)}\frac{1}{V-V_c}[P_{A,0} + P_{B,0}\frac{V_\lambda}{V}], \qquad (9)$$

where $x \approx N$ means that the translocation process starts near the *cis*-side of the membrane.

Equation 9 provides a good description of the numerically obtained dependence of the translocation velocity on the voltage. $\langle\tau\rangle$ consists of two terms that can be attributed to the A (*first term in the brackets*) and B (*second term in the brackets*) pore conformations. For $V_\lambda \approx 120$ mV we can replace the expression in brackets by unity in the relevant voltages window. Thus, we find that $\langle\tau\rangle \propto (V-V_C)^{-1}$, which implies that $F(t)$ has one translocation peak for this choice of V_λ. For higher values of V_λ and voltages of biological interest, the two terms in the brackets contribute separately. This leads to a term that represent the A conformation and scales as $(V-V_C)^{-1}$, and a term that represents the B conformation that scales as $[V(V-V_C)]^{-1}$.

Accordingly, Eq. 9 captures the physical essence of the translocation of the ssDNA through the conformationally changing pore, under a relatively small field.

Field-free translocation

In recent field-free experiments by Bates et al. (2003), the cdf $G(t) = \int_0^t F(s)ds$ was shown to have two regimes that were approximated by a fast and a slow timescales, τ_1 and τ_2, with the ratio $\tau_1/\tau_2 \approx 1{:}20$.

Motivated by these experimental results, which implies, within our approach, that λ_0 fulfills $\lambda_0 \ll 1$, we study in this subsection the zero field translocation, $V \to 0$. We start by computing $G(t)$ for a translocation process that starts at the middle state, $x = n/2$. This is the same initial condition that was imposed in the experiments (Bates et al., 2003). As shown in Fig. 5 (*full curve*), $G(t)$ displays two regimes, a fast increase at short times and a slow increase from intermediate to large times. Accordingly, we try the approximation

$$G_{ap}(t) \approx 1 - (P_{A,0}e^{-t/\tau_1} + P_{B,0}e^{-t/\tau_2}). \qquad (10)$$

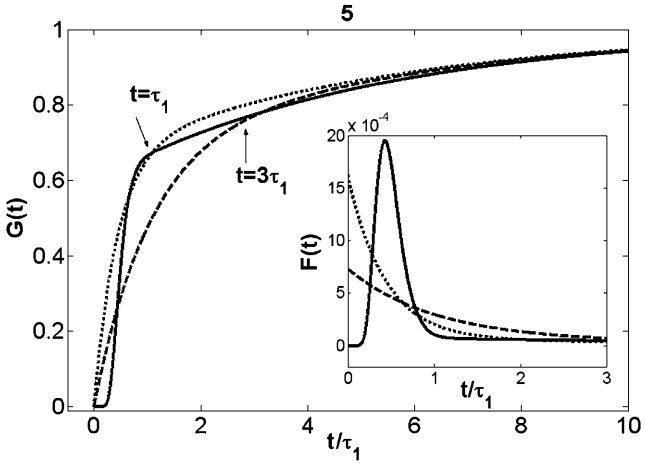

FIGURE 5 $G(t)$ for poly-dA_{nu} (*full curve*) for $V = 0$, and the initial state $x = n/2$, $\omega_A = 10^{-2}$ Hz, $\omega = 1/2$ and the other parameters as in Fig. 1. Also shown is the approximate cdf $G_{ap}(t)$ (*dashed curve*) and its modified version (*dotted curve*). (*Inset*) $F(t)$ for poly-dA_{nu} for the corresponding cdf shown in the main figure.

Identifying the first and the second moments obtained from $F(t)$ with those from the approximate $F(t)$ we find that the characteristics timescales of $G_{ap}(t)$ are (see Appendix D)

$$\tau_1 = \bar{\tau}(1 + 3\omega/2); \quad \tau_2 = \bar{\tau}(1/2 + \omega) + 1/\omega_B, \qquad (11)$$

which, when used in $G_{ap}(t)$, lead to the dashed curve plotted in Fig. 5. Also shown, by dotted curve, is a modified version of $G_{ap}(t)$, where $\tau_1 \to t_m$ is used in Eq. 10. Note that for the short times, $t < \tau_1$, the latter approximation fits $G(t)$ better, but from intermediate times, $t > 3\tau_1$, $G_{ap}(t)$, and $G(t)$ coincide.

The two-conformation model produces a temporal behavior that agrees with experimental observation, and provides a good explanation for it. In the limit, $V \to 0$, the B conformation acts as a trapping conformation; namely, the polymer is stuck in its position when subject to the environment due to the B conformation. Movement occurs only through the A conformation. As a result two regimes are obtained for $G(t)$. The fast increase in $G(t)$ at short times is a consequence of exiting due to the A conformation (at either side of the membrane), whereas the slow saturation at longer times is a result of the release from the trapping in the B conformation.

In the inset of Fig. 5 we show both $F(t)$, the approximate $F(t)$, and the modified version of the approximation, which is obtained when using $\tau_1 \to t_m$. Because the process starts in the middle state, $x = n/2$, $F(t)$ has only one peak, which coincides with previous results (Flomenbom and Klafter, 2003). Although the approximate $F(t)$ or any other approximation of two exponentials with positive coefficients does not exhibit a peaked shape, information about the maximal peak value of $F(t)$ and the interconversion rates can

still be extracted from $G_{ap}(t)$ timescales by using Eq. 11. For example, the timescales suggested by Bates et al. (2003) imply that $t_m \approx 165\ \mu s$ and $\omega_B \approx 300$ Hz.

CONCLUSIONS

The model introduced here describes the translocation of ssDNA through a fluctuating pore structure. As a consequence the ssDNA within the transmembrane pore part is exposed to a changing environment, which could be reflected in the first passage times pdf, $F(t)$. By computing $F(t)$, comparing our results to experimental observations, and using physical arguments, we obtained theoretically a behavior which was previously observed experimentally $-F(t)$ having three peaks. This behavior is obtained by tuning the dimensionless parameter λ, which controls the effect of the change in the pore structure on the translocating ssDNA, and the interconversion rates between the pore conformations, ω_A and ω_B. In particular, λ has to fulfill $0.10 \leq \lambda \leq 0.30$, and the interconversions rates have to be of the same order of magnitude, and much smaller than the typical rate of the A pore conformation, k, $\omega_B/k \leq 10^{-3}$. This implies that the relaxation timescale of the ssDNA in the pore is much shorter than the pore-conformational change timescale. From these conditions the maximal values of the interconversion rates can be deduced from the value of k, given by Eq. 3, to be $\omega_A \approx \omega_B = 10^2$ Hz.

We have been able to show, both numerically and analytically, that the times that maximize the actual translocation peaks, $t_{m,i}$, $i = 2, 3$, and the MFPT, are inversely proportional to the first or the second power of the field, depending on V_λ. This emphasizes the crucial role played by V_λ in the translocation process, and may explain the different experimental results for $F(t)$ discussed in the introduction, meaning that V_λ is sensitive to the specific experimental setup and biological conditions.

The probability to exit the channel until time t, $G(t)$, in a field-free environment, has been shown to have two regimes that can be approximated by two timescales, τ_1 and τ_2, which are approximately one order-of-magnitude apart, and are closely related to the $\bar{\tau}$, t_m, and the interconversion rates: $\tau_1 = \bar{\tau}(1 + 3\omega/2)$ or $\tau_1 \to t_m$, and $\tau_2 = \bar{\tau}(1/2 + \omega) + 1/\omega_B$. From these relations the interconversion rates can be deduced when analyzing experimental data.

APPENDIX A

In this Appendix we introduce the formal solution of Eq. 6 and define the symbols used in next derivations. In general, $S(t)$ for a discrete system is given by summing the elements of the vector that solves the ME,

$$S(t) = \vec{U}_{2n}\mathbf{E}e^{\mathbf{D}t}\mathbf{E}^{-1}\vec{P}(0|2n). \tag{A1}$$

Here $\vec{U}_{2n}$ is the summation row vector of $2n$ dimensions, $\vec{P}(0|2n)$ is the initial condition column vector, and

$$[\vec{P}(0|2n)]_j = (P_{A,0}\delta_{x,j} + P_{B,0}\delta_{x+n,j}), \tag{A2}$$

where x is the initial state of the translocation process. The definite negative real part eigenvalues matrix, $\mathbf{D}$, is obtained through the similarity transformation of $\mathbf{D} = \mathbf{E}^{-1}\mathbf{H}\mathbf{E}$, where $\mathbf{H}$ is the matrix given on the right-hand side of Eq. 6, and $\mathbf{E}$ and $\mathbf{E}^{-1}$ are the eigenvectors matrix, and the inverse, of $\mathbf{H}$.

APPENDIX B

Here we calculate formally the MFPT $\langle\tau\rangle$. The m moment of $F(t)$ is given by $\langle t^m\rangle = \int_0^\infty t^m F(t)dt = m!\vec{U}_{2n}(-\mathbf{H})^{-m}\vec{P}(0|2n)$ to calculate the inverse of the propagation matrix $\mathbf{H}$, which is given on the right-hand side of Eq. 6. We use the projection operator of Klafter and Silbey (1980) and Zwanzig (2001), $\mathbf{QHQ} \equiv \mathbf{H_{QQ}} = \mathbf{A} - \omega_A$, $\mathbf{H_{QZ}} = \omega_B$, $\mathbf{H_{ZQ}} = \omega_A$, $\mathbf{H_{ZZ}} = \mathbf{B} - \omega_B$, and the identity, $\mathbf{I} = \mathbf{HM}$, and obtain $\mathbf{M}$ blocks,

$$\begin{aligned}\mathbf{M_{QQ}} &= [\mathbf{A_{QQ}} - \mathbf{A_{QZ}}(\mathbf{A_{ZZ}})^{-1}\mathbf{A_{ZQ}}]^{-1} = \mathbf{A}^{-1}\mathbf{C}(\mathbf{B} - \boldsymbol{\omega}_\mathbf{B})\\ \mathbf{M_{QZ}} &= [\mathbf{A_{ZQ}} - \mathbf{A_{ZZ}}(\mathbf{A_{QZ}})^{-1}\mathbf{A_{QQ}}]^{-1} = -\mathbf{A}^{-1}\mathbf{C}\boldsymbol{\omega}_\mathbf{B},\end{aligned} \tag{B1}$$

where $\mathbf{M_{ZQ}}$ and $\mathbf{M_{ZZ}}$ are obtained in a similar way. Now, we can write the m moment vector of $F(t)$ as

$$\langle\vec{t^m}\rangle = m!(-\mathbf{M})^m\vec{P}(0|2n), \tag{B2}$$

where $\mathbf{M}$ is given by

$$\mathbf{M} = \begin{pmatrix} \mathbf{A}^{-1}\mathbf{C}(\mathbf{B} - \omega_\mathbf{B}) & -\mathbf{A}^{-1}\mathbf{C}\omega_\mathbf{B} \\ -\mathbf{A}^{-1}\mathbf{C}\omega_\mathbf{A} & \mathbf{A}^{-1}\mathbf{C}(\mathbf{A} - \omega_\mathbf{A}) \end{pmatrix}, \tag{B3}$$

and $\mathbf{C} = (\mathbf{B} - \omega_\mathbf{B} - \lambda\omega_\mathbf{A})^{-1}$. For $m = 1$ in Eq. B2 we obtain the MFPT vector

$$\langle\vec{\tau}\rangle = \begin{pmatrix} -\mathbf{A}^{-1}\mathbf{C}(P_{A,0}\mathbf{B} - \omega_\mathbf{B})\vec{P}(0|n) \\ -\mathbf{A}^{-1}\mathbf{C}(P_{B,0}\mathbf{A} - \omega_\mathbf{A})\vec{P}(0|n) \end{pmatrix}, \tag{B4}$$

where $[\vec{P}(0|n)]_j = \delta_{x,j}$. Summing $\langle\vec{\tau}\rangle$ elements by using the summation row vector of n dimensions $\vec{U}_n$, results in

$$\begin{aligned}\langle\tau\rangle = &-\vec{U}_n\mathbf{C}\vec{P}(0|n)(\lambda P_{A,0} + P_{B,0})\\ &+ \vec{U}_n\mathbf{A}^{-1}\mathbf{C}\vec{P}(0|n)(\omega_A + \omega_B).\end{aligned} \tag{B5}$$

Note that the MFPT of the single A conformation, $\bar{\tau}$, is $\bar{\tau} = -\vec{U}_n\mathbf{A}^{-1}\vec{P}(0|n)$, which has a similar form to the first term in Eq. B5 when choosing $\mathbf{C}^{-1}$ as the propagation matrix.

It is easy to verify that for $\lambda = 1$, $\langle\tau\rangle$ reduces to the MFPT of the single conformation case, $\bar{\tau}$. Rewriting Eq. B5 as

$$\langle\tau\rangle = -\vec{U}_n\mathbf{A}^{-1}\mathbf{C}[P_{A,0}\mathbf{B} + P_{B,0}\mathbf{A} - \omega_\mathbf{A} - \omega_\mathbf{B}]\vec{P}(0|n) \tag{B6}$$

and substituting $\lambda = 1$, we find that

$$\langle\tau\rangle = -\vec{U}_n\mathbf{A}^{-1}\vec{P}(0|n) = \bar{\tau}. \tag{B7}$$

APPENDIX C

To obtain an explicit expression for the MFPT of the translocation in a weak field limit, we first rewrite Eq. B5 as

$$\langle\tau\rangle = \hat{\tau}(\lambda P_{A,0} + P_{B,0}) + \tilde{\sigma^2}(\omega_A + \omega_B), \tag{C1}$$

where $\hat{\boldsymbol{\tau}} = -\vec{U}_n \mathbf{C} \vec{P}(0|n)$ and $\tilde{\boldsymbol{\sigma}}^2 = \vec{U}_n \mathbf{A}^{-1} \mathbf{C} \vec{P}(0|n)$. We can further rewrite $\hat{\boldsymbol{\tau}}$ as $\hat{\boldsymbol{\tau}} = \sum_{s=1}^{n} \hat{\boldsymbol{\tau}}_{s,x}$, where $\hat{\boldsymbol{\tau}}_{s,x} \equiv -(\mathbf{C})_{s,x}$ defines the mean residence time spent in state s before exiting the channel, given that the process started at state x (Bar-Haim and Klafter, 1998), and has the form (Huang and McColl, 1997) of

$$-(\mathbf{C})_{s,x} = \frac{\Delta(h^s)\Delta(h^{n+1-x}) r^{x-s}}{\Delta(h)\Delta(h^{n+1})\hat{k}}; \quad s < x, \tag{C2}$$

where $(\mathbf{C})_{s,x}$ for $s \geq x$ is obtained when exchanging x for s and r for l in Eq. C2. Here $h_{\pm} = [1 \pm (1\text{–}4rl)^{1/2}]/2$, $r = ap_+$, $l = ap_-$, $a = \lambda k/\hat{k}$, and $\hat{k} = \lambda k + \omega_B + \lambda\omega_A$. Thus, we find that $\hat{\boldsymbol{\tau}}_{s,x}$ is a function of the parameter $a = [1 + (\omega_A + \omega_B/\lambda)/k]^{-1}$, which obeys $0 \leq a \leq 1$, and is a measure of the difference between $\bar{\boldsymbol{\tau}}$ and $\hat{\boldsymbol{\tau}}$. Using $\omega \approx 1$ and $\omega_A/k \approx 10^{-3}$ leads to $a \approx 1$ given $V/V_C \geq 1$, and accordingly to

$$(\mathbf{C})_{s,x} = (\mathbf{A}^{-1})_{s,x} k/\hat{k} = (\mathbf{A}^{-1})_{s,x}/\lambda, \tag{C3}$$

where Eq. C3 implies

$$\hat{\boldsymbol{\tau}} = \bar{\boldsymbol{\tau}}/\lambda. \tag{C4}$$

To obtain an explicit expression for $\bar{\boldsymbol{\tau}}$, it is convenient to use the independence approximation and replace $p_{j,j-1}$ and k_j by state-independent terms: $p_+ = [1 + e^{(-V/V_c+1)}]^{-1}$ and k. This approximation, which is valid for large polymers, $N > d$, and which becomes more accurate as N increases, leads to $a_+ = p_+ k$, $a_- = (1 - p_+)k$, so that (Flomenbom and Klafter, 2003),

$$\bar{\boldsymbol{\tau}} = \frac{\Delta(p^{n+1-x})p_+^x x - \Delta(p^x)p_-^{n+1-x}(n+1-x)}{k\Delta p \Delta(p^{n+1})}, \tag{C5}$$

where $\Delta(p^s) = p_+^s - p_-^s$. In the limit of a not-too-large field, $V/V_C \gtrsim 1$, Eq. C5 reduces to

$$\bar{\boldsymbol{\tau}} \approx \frac{2x\xi_p b^2 d^{\mu}}{z|q|(1+1/d)} \frac{1}{V - V_C}. \tag{C6}$$

To compute $\tilde{\boldsymbol{\sigma}}^2$ we rewrite $\tilde{\boldsymbol{\sigma}}^2$ as $\tilde{\boldsymbol{\sigma}}^2 = \sum_{s=1}^{n} \bar{\boldsymbol{\tau}}_s \hat{\boldsymbol{\tau}}_{s,x}$, where $\bar{\boldsymbol{\tau}}_s$ is given by Eq. C5 for $x = s$, and $\hat{\boldsymbol{\tau}}_{s,x}$ is given by Eq. C2. For $a \approx 1$ we have $\tilde{\boldsymbol{\sigma}}^2 = \overline{\boldsymbol{\tau}^2}/2\lambda$, where $\overline{\boldsymbol{\tau}^2}$ is the second moment of $F(t)$ for the single A conformation case. The calculation of $\overline{\boldsymbol{\tau}^2}/2 = \sum_{s=1}^{n} \bar{\boldsymbol{\tau}}_s \bar{\boldsymbol{\tau}}_{s,x}$ yields in the weak field limit $V/V_C \gtrsim 1$,

$$\frac{\overline{\boldsymbol{\tau}^2}}{2} \approx \frac{1}{(k\Delta p)^2}\left[\frac{x(x-1)}{2} + \frac{xy^x(1-y) - y(1-y^x)}{(1-y)^2} + II\right], \tag{C7}$$

where $y = p_-/p_+$ and

$$II = \frac{y^{-x} - 1}{y^{-n} - 1}\left[\frac{p_-^{x-n-1}}{1/p_- - 1}\left(\frac{p_+^{n+1-x} - 1}{1 - p_+} + n + 1 - x p_+^{n+1-x}\right) - (n+1-x)\frac{n+x}{2}\right]. \tag{C8}$$

Noticing that II represents the nontranslocation events and vanishes for $V/V_C \gtrsim 1$ as y^{n-x}, we rewrite Eq. C7 up to a leading term in x as

$$\frac{\overline{\boldsymbol{\tau}^2}}{2} \approx \frac{x(x-1)}{2(k\Delta p)^2}. \tag{C9}$$

Using $\bar{\boldsymbol{\tau}} \approx (x/k\Delta p)$ valid for $V/V_C \gtrsim 1$ (Flomenbom and Klafter, 2003), Eq. C9 yields for a leading order in x,

$$\tilde{\boldsymbol{\sigma}}^2 \approx \bar{\boldsymbol{\tau}}^2/2\lambda. \tag{C10}$$

Substituting Eq. C4 and Eq. C10 into Eq. C1, Eq. 8 is obtained.

APPENDIX D

For the analysis of the field-free translocation we start by computing $\langle\tau\rangle$ and $\langle\tau^2\rangle$. Substituting $\lambda = 0$ in Eq. B5, we obtain

$$\langle\tau\rangle = -\vec{U}_n \mathbf{A}^{-1} \vec{P}_n(0)\left(\frac{\omega_A + \omega_B}{\omega_B}\right) + \frac{P_{B,0}}{\omega_B}, \tag{D1}$$

which can be written as

$$\langle\tau\rangle = \bar{\boldsymbol{\tau}}(1+\omega) + P_{B,0}/\omega_B. \tag{D2}$$

Note that experiments suggest that $\lambda_0 \ll 1$, which leads to $\lambda_0 k < \omega_B$, whereas $\lambda_0 k \ll \omega_B$ is used for simplification, and enables the substitution of $\lambda = 0$ in Eq. B5.

To compute $\langle\tau^2\rangle$, we have to calculate the blocks of $\mathbf{M}^2$,

$$\begin{aligned}
\mathbf{M}^2_{QQ} &= \mathbf{A}^{-2}(1+\omega);\\
\mathbf{M}^2_{QZ} &= \mathbf{A}^{-2}(1+\omega) - \mathbf{A}^{-1}/\omega_B;\\
\mathbf{M}^2_{ZQ} &= \mathbf{A}^{-2}\omega(1+\omega);\\
\mathbf{M}^2_{ZZ} &= \mathbf{A}^{-2}\omega(1+\omega) - \mathbf{A}^{-1}2\omega/\omega_B + 1/\boldsymbol{\omega}_B^2.
\end{aligned} \tag{D3}$$

Substituting Eq. D3 into Eq. B2 and summing the vector elements, we obtain

$$\frac{\langle\tau^2\rangle}{2} = \frac{\overline{\boldsymbol{\tau}^2}}{2}(1+\omega)^2 + \bar{\boldsymbol{\tau}}(1+2\omega)\frac{P_{B,0}}{\omega_B} + \frac{P_{B,0}}{\omega_B^2}. \tag{D4}$$

To get the relaxation timescales of $G_{ap}(t)$, τ_1, and τ_2, we identify $\langle\tau\rangle$ and $\langle\tau^2\rangle$ obtained from

$$F_{ap}(t) = \frac{P_{A,0}}{\tau_1} e^{-t/\tau_1} + \frac{P_{B,0}}{\tau_2} e^{-t/\tau_2}, \tag{D5}$$

with the corresponding moments obtained from Eq. D2 and Eq. D4. This procedure yields

$$\tau_1 = \frac{\langle\tau\rangle - P_{B,0}\tau_2}{P_{A,0}}, \tag{D6}$$

and

$$\tau_2 = \langle\tau\rangle + \left[\frac{P_{A,0}}{P_{B,0}}\left(\frac{\langle\tau^2\rangle}{2} - \langle\tau\rangle^2\right)\right]^{1/2}. \tag{D7}$$

Substituting Eq. D2 and Eq. D4 into Eq. D7 results in

$$\tau_z = \bar{\boldsymbol{\tau}}(1+\omega) + \frac{P_{B,0}}{\omega_B} + \frac{P_{A,0}}{\omega_B} \times \left[1 - \bar{\boldsymbol{\tau}}\frac{\omega_B}{P_{A,0}} + \frac{\omega_B^2}{P_{A,0}P_{B,0}}\left(\frac{\overline{\boldsymbol{\tau}^2}}{2} - \bar{\boldsymbol{\tau}}^2\right)\right]^{1/2}. \tag{D8}$$

Expanding the square root in Eq. D8 to leading order and using Eq. D6, Eq. 11 is obtained.

APPENDIX E

TABLE 1 Abbreviations

Symbol	Definition	Expression
N	Number of monomers in the polymer	
d	Channel length in monomer length units	
n	System length	$n = N + d–1$
x	Initial state of the translocation process	
b	Monomer length	
ξ_p	ssDNA-TPP interaction coefficient	
μ	Rigidity coefficient of the ssDNA inside the TPP	
k	Dominant rate of conformation A	$k = 1/(\beta\xi_p b^2 d^\mu)$
zq	Effective charge per monomer	
V_C	Characteristic voltage of the translocation	$V_C = 1/[\beta z\|q\|(1 + 1/d)]$
λ	Effective parameter of conformational change	$\lambda \approx \lambda_0 + V/V_\lambda$
ω_A	Rate of change from conformation A to B	
ω_B	Rate of change from conformation B to A	
ω	Ratio between the conformational change rates	$\omega = \omega_A/\omega_B$
$P_{A,0}$	Initial occupancy probability of conformation A	$P_{A,0} = \frac{\omega_B}{\omega_A + \omega_B}$
$P_{B,0}$	Initial occupancy probability of conformation B	$P_{B,0} = \frac{\omega_A}{\omega_A + \omega_B}$
$F(t)$	Translocation FPT pdf	
$t_{m,i}$	Time that maximizes the i^{th} $F(t)$ peak	
$\overline{\tau}$	MFPT for the single conformation case	$\overline{\tau} \approx \frac{2x\xi_p b^2 d^\mu}{z\|q\|(1+1/d)} \frac{1}{V - V_c}$
$\langle\tau\rangle$	MFPT for the two-conformation case	$\langle\tau\rangle \approx \overline{\tau}(P_{A,0} + \frac{V_\lambda P_{B,0}}{V})$
$G(t)$	The translocation FPT cdf	$G(t) = \int_0^t F(s)ds$
τ_1	$P_{A,0}$ weighted timescale of $G(t)$	$\tau_1 = \overline{\tau}(1 + 3\omega/2)$
τ_2	$P_{B,0}$ weighted timescale of $G(t)$	$\tau_2 = \overline{\tau}(1/2 + \omega) + 1/\omega_B$

We acknowledge fruitful discussions with Ralf Metzler and with Amit Meller.

We acknowledge the support of the United States-Israel Binational Science Foundation and the Tel-Aviv University Nanotechnology Center.

REFERENCES

Alberts, B., K. Roberts, D. Bray, J. Lewis, M. Raff, and J. D. Watson. 1994. Molecular Biology of The Cell. Garland Publishing, New York and London.

Ambjornsson, T., S. P. Apell, Z. Konkoli, E. A. Di Marzio, and J. J. Kasianowicz. 2002. Charged polymer membrane translocation. *J. Chem. Phys.* 117:4063–4073.

Bar-Haim, A., and J. Klafter. 1998. On mean residence and first passage times in finite one-dimensional systems. *J. Chem. Phys.* 109:5187–5193.

Bar-Haim, A., and J. Klafter. 1999. Escape from a fluctuating system: a master equation and trapping approach. *Phys. Rev. E.* 60:2554–2558.

Bates, M., M. Burns, and A. Meller. 2003. Dynamics of DNA molecules in a membrane channel probed by active control techniques. *Biophys. J.* 84:2366–2372.

Berezhkovskii, A. M., and I. V. Gopich. 2003. Translocation of rodlike polymers through membrane channels. *Biophys. J.* 84:787–793.

Chuang, J., Y. Kantor, and M. Kardar. 2001. Anomalous dynamics of translocation. *Phys. Rev. E.* 65:011802–011808.

Doering, C. R., and J. C. Gadoua. 1992. Resonant activation over a fluctuating barrier. *Phys. Rev. Lett.* 69:2318–2321.

Doi, M., and S. F. Edwards. 1986. The Theory of Polymer Dynamics. Clarendon Press, Oxford, UK.

Huang, Y., and W. F. McColl. 1997. Analytical inversion of general tridiagonal matrices. *J. Phys. A.* 30:7919–7933.

Flomenbom, O., and J. Klafter. 2003. Single-stranded DNA translocation through a nanopore: a master equation approach. *Phys. Rev. E.* 68: 041910–041917.

Flomenbom, O., and J. Klafter. 2004. Insight into resonant activation in discrete systems. *Phys. Rev. E.* 69:5. In press. Appeared on: http://xxx.lanl.gov/abs/cond-mat/0402331.

Kasianowicz, J. J., E. Brandin, D. Branton, and D. W. Deamer. 1996. Characterization of individual polynucleotide molecules using a membrane channel. *Proc. Natl. Acad. Sci. USA.* 93:13770–13773.

Klafter, J., and R. Silbey. 1980. Derivation of the continuous-time random-walk equation. *Phys. Rev. Lett.* 44:55–58.

Kafri, Y., D. K. Lubensky, and D. R. Nelson. 2004. Dynamics of molecular motors and polymer translocation with sequence heterogeneity. *Biophys. J.* 86:3373–3391. Appeared on: http://xxx.lanl.gov/abs/cond-mat/0310455.

Lubensky, D. K., and D. R. Nelson. 2001. Driven polymer translocation through a narrow pore. *Biophys. J.* 77:1824–1838.

Madigan, M. T., J. M. Matinko, and J. Parker. 1997. Biology of Microorganisms. Prentice-Hall, Englewood Cliffs, NJ.

Meller, A. 2003. Dynamics of polynucleotide transport through nanometer-scale pores. *J. Phys. Cond. Matt.* 15:R581–R607.

Meller, A., L. Nivon, and D. Branton. 2001. Voltage-driven DNA translocations through a nanopore. *Phys. Rev. Lett.* 86:3435–3438.

Metzler, R., and J. Klafter. 2003. When translocation dynamics becomes anomalous. *Biophys. J.* 85:2776–2779.

Muthukumar, M. 1999. Polymer translocation through a hole. *J. Chem. Phys.* 111:10371–10374.

Redner, S. 2001. A Guide to First-Passage Process. Cambridge University Press, Cambridge, UK.

Slonika, E., and A. B. Kolomeisky. 2003. Charged polymer membrane translocation. *J. Chem. Phys.* 118:7112–7118.

Slutsky, M., M. Kardar, and L. A. Mirny. 2004. Diffusion in correlated random potentials, with applications to DNA. *Phys. Rev. E.* In press. Appeared on: http://xxx.lanl.gov/abs/q-bio.BM/0310008.

Song, L., M. R. Hobaugh, C. Shustak, S. Cheley, H. Balyley, and J. E. Gouaux. 1996. Structure of staphylococcal α-hemolysin, a heptameric transmembrane pore. *Science.* 274:1859–1866.

Sung, W., and P. J. Park. 1996. Polymer translocation through a pore in a membrane. *Phys. Rev. Lett.* 77:783–786.

Zwanzig, R. 2001. Nonequilibrium Statistical Mechanics. Oxford University Press, NY, NY.